Diastolic Dysfunction in Women With Signs and Symptoms of Ischemia in the Absence of Obstructive Coronary Artery Disease

A Hypothesis-Generating Study

Michael D. Nelson, PhD; Lidia S. Szczepaniak, PhD; Janet Wei, MD; Afsaneh Haftabaradaren, MD; Meghan Bharadwaj, BA; Behzad Sharif, PhD; Puja Mehta, MD; Xiao Zhang, PhD; Louise E. Thomson, MD; Daniel S. Berman, MD; Debiao Li, PhD; C. Noel Bairey Merz, MD

Background—Angina, in the absence of obstructive coronary artery disease, is more common in women, is associated with adverse cardiovascular morbidity and mortality, and is a major burden to the healthcare system. Although advancements have been made to understand the mechanistic underpinning of this disease, the functional consequence remains unclear.

Methods and Results—Cardiac magnetic resonance imaging was performed to assess left ventricular function in 20 women with signs and symptoms of ischemia, but no obstructive coronary artery disease (cases), and 15 age- and body mass index–matched reference controls. Functional imaging included standard cinematic imaging to assess left ventricular morphology and global function, along with tissue tagging to assess left ventricular tissue deformation. Systolic function was preserved in both cases and controls, with no differences in ejection fraction (mean±SE: 63.1±8% versus 65±2%), circumferential strain (−20.7±0.6% versus −21.9±0.5%), or systolic circumferential strain rate (−105.9±6.1% versus −109.0±3.8% per second). In contrast, we observed significant differences between cases and controls in diastolic function, as demonstrated by reductions in both diastolic circumferential strain rate (153.8±8.9% versus 191.4±8.9% per second; $P<0.05$) and peak rate of left ventricular untwisting (−99.4±8.0° versus −129.4±12.8° per second; $P<0.05$).

Conclusions—Diastolic function is impaired in women with signs and symptoms of ischemia in the absence of coronary artery disease, as assessed by cardiac magnetic resonance tissue tagging. These results are hypothesis-generating. Larger studies are needed to define the exact mechanism(s) responsible and to establish viable treatment strategies. **(*Circ Cardiovasc Imaging*. 2014;7:510-516.)**

Key Words: diastole ■ magnetic resonance imaging ■ myocardial ischemia ■ women

Signs and symptoms of ischemia in the absence of obstructive coronary artery disease (CAD) represent an important clinical problem, especially for women. Indeed, women with signs and symptoms of ischemia, but without obstructive CAD, are at increased risk for adverse cardiovascular events compared with asymptomatic community-based women.[1] Moreover, symptom-driven health care is costly, with average lifetime cost estimates of >$750 000.[2]

Editorial see p 420
Clinical Perspective on p 516

The Women's Ischemia Syndrome Evaluation (WISE), designed to investigate new and innovative techniques for the detection of ischemic heart disease in women,[3] described an abnormal metabolic response to mild stress testing using ^{31}P magnetic resonance (MR) spectroscopy in women with signs and symptoms of ischemia but no obstructive CAD.[4] We and others have subsequently found this abnormality to be related to abnormal coronary reactivity,[5,6] microvascular coronary dysfunction,[7,8] and plaque erosion/distal microembolization.[9,10] Despite this background, it remains unclear whether these abnormalities manifest into actual changes in ventricular function.

Accordingly, we incorporated MR tissue tagging into our standard MR imaging protocol to assess left ventricular (LV) systolic and diastolic function. MR tissue tagging is an accurate noninvasive imaging technique that provides detailed quantitative information about myocardial tissue deformation.[11,12] The application of this technique to a variety of different diseases has allowed for the early detection of subclinical LV dysfunction[13,14] and, more recently, for the assessment of diastolic function.[15,16] We hypothesized that women with angina in the absence of obstructive CAD would have

Received November 27, 2013; accepted March 10, 2014.

From the Heart Institute (M.D.N., C.N.B.M.), Biomedical Imaging Research Institute (L.S.S., B.S., D.L.), Diabetes and Obesity Research Institute (L.S.S.), Barbra Streisand Women's Heart Center (J.W., A.H., M.B., P.M., C.N.B.M.), Biostatistics and Bioinformatics Research Center (X.Z.), and S. Mark Taper Foundation Imaging Center (L.E.T., D. S. B.), Cedars-Sinai Medical Center, Los Angeles, CA.

Correspondence to Michael D. Nelson, PhD, Cedars-Sinai Heart Institute, 8700 Beverly Blvd, Los Angeles, CA 90048. E-mail michael.nelson@cshs.org

Circ Cardiovasc Imaging **is available at http://circimaging.ahajournals.org** **DOI: 10.1161/CIRCIMAGING.114.001714**

impaired diastolic function, but preserved systolic function, compared with a group of age-matched reference controls.

Methods

Study Population

The population consisted of 20 women (median age, 60 years) who were evaluated at Cedars-Sinai Medical Center for signs and symptoms of ischemia and had no obstructive CAD (defined as coronary stenosis of >20% in any epicardial coronary artery). Women were enrolled in the National Heart, Lung, and Blood Institute–sponsored WISE-Cardiovascular Dysfunction Study, and their coronary angiograms were reviewed by the angiographic core laboratory. These women underwent cardiac MR imaging (MRI) for LV function and perfusion imaging.[3] Exclusion criteria included acute myocardial infarction <30 days, planned percutaneous intervention or coronary bypass surgery, primary valvular disease, cardiogenic shock or intra-aortic balloon pump, New York Heart Association class III or IV heart failure, ejection fraction <40%, hypertrophic cardiomyopathy, severe renal or liver disease, pregnancy, life expectancy <6 months, and contraindications to angiography (hypersensitivity to contrast, active bleeding, bleeding diathesis, renal dysfunction). A reference control group of 15 women (median age, 56 years) was also recruited to serve as control subjects for the MRI. The reference control group had no cardiac risk factors according to the National Cholesterol Education Program guidelines,[17] had no evidence of heart disease on the basis of a normal maximal exercise treadmill stress testing (Bruce protocol), and did not possess any of the clinical conditions described in the exclusion criteria above. All subjects provided informed consent, and their physicians approved their participation.

MRI

Cardiac MRI was performed in the supine position on a 1.5-T MR scanner (Avanto; Siemens Healthcare, Erlangen, Germany) with ECG gating and a phased-array surface coil (CP Body Array Flex; Siemens Healthcare). A highly standardized protocol was used and included assessment of LV morphology and function, in addition to pharmacological stress and rest first-pass myocardial perfusion imaging with a total gadolinium-based contrast dose of 0.1 mmol/kg (Optimark; Mallinckrodt, St Louis, MO). Blood pressure and pulse oxygenation were monitored (Invivo, Philadelphia, PA) and recorded before, during, and after adenosine infusion. A 12-lead ECG was recorded before and after MRI. Subjects had caffeine withdrawn for ≈24 hours before the examination.

LV Function

Breath-hold cine MRI using balanced steady-state free precession was acquired covering the left ventricle with a stack of 10 to 12 short-axis slices from base to apex, as well as one 4-chamber long-axis and one 2-chamber long-axis image (field of view, 350 mm; temporal resolution, 44.4 ms; echo spacing, 3.2 ms; echo time, 1.3 ms; flip angle, 80°; slice thickness, 8.0 mm; 2 mm gap; 25 cardiac phases; 2-fold TGRAPPA parallel imaging). Tagged short-axis images were also acquired using a gradient echo sequence (breath-hold scan; field of view, 400 mm; temporal resolution, 19.6 ms; echo spacing, 4.0 ms; echo time, 2.78 ms; flip angle, 14°; slice thickness, 8.0 mm; 2-fold TGRAPPA parallel imaging). Two sets of scans for 4 adjacent short-axis slices were acquired, covering the entire left ventricle from base to apex. The first set of grid tags focused on systolic function by triggering the tagging sequence at end-diastole (R wave of ECG). Tissue tags fade after ≈400 to 500 ms due to T1 relaxation,[18] which could adversely affect the interpretation of diastolic indices that normally occur at this time. To overcome this potential limitation, we acquired a second set of grid tags with a trigger delay set to end-systole (defined as the smallest ventricular cavity area), thus ensuring optional tag quality throughout diastole.

LV Perfusion and Delayed Enhancement Imaging

As previously described,[19] the LV short axis was determined by scout imaging, and first-pass perfusion images were obtained in basal, mid, and distal short-axis image planes. A gradient echo-echo planar imaging hybrid pulse sequence was used for all patients (field of view, 350×350 mm^2 or minimized dependent on patient size; slice thickness, 8 mm; TR/TE maximum, 6.5/1.3 ms; receiver bandwidth, 1420 Hz/pixel; 2-fold TGRAPPA parallel imaging; temporal resolution, 1 heartbeat). For pharmacological stress, adenosine (Adenoscan; Astellas Pharma US, Inc, Northbrook, IL) was injected at a dose of 140 μg/kg per minute intravenously over a total duration of 4 minutes. Then 0.05 mmol/kg of Gd-DTPA was administered (2 minutes later) via a second intravenous catheter at a rate of 4 mL/s, followed by 30 mL saline flush at the same rate. After a 10-minute wait to allow for contrast washout, rest perfusion imaging was performed with the same contrast settings. Delayed contrast enhancement images—10 to 12 short-axis slices, 1 horizontal long-axis slice, and 1 vertical long-axis slice at the same positions as the LV function cine images—were obtained 10 minutes after to identify regional fibrosis.

MRI Analysis

Using commercially available software (CAAS MRV 3.3; Pie Medical Imaging B.V., Maastricht, the Netherlands), LV mass, LV volume, and LV early peak filling rate and time to peak filling rate were assessed by manually tracing the epicardial and endocardial borders of the short-axis cine images as previously described.[20–22] Stroke volume was calculated as end-diastolic volume minus end-systolic volume. Ejection fraction was calculated as stroke volume divided by end-diastolic volume. LV mass was indexed to end-diastolic volume to evaluate LV concentricity.

As illustrated in conceptual Figure 1, tissue tagging analysis was performed by manually tracing the epicardial and endocardial borders of each slice, using commercially available software (HARP; Diagnosoft). Circumferential strain and its time derivative in systole and diastole were calculated, along with the peak rate of rotation across the 2 most distal LV slices (base and apex) in diastole (referred to as the peak untwisting rate). Our in-laboratory intrarater reliability for measuring peak circumferential strain, systolic circumferential strain rate, diastolic circumferential strain rate, and peak untwisting rate, reported as a coefficient of variation, is 2.1%, 3.6%, 4.2%, and 4.3%, respectively.

Quantitative analysis of the first-pass perfusion images for the assessment of myocardial perfusion reserve index (MPRI) was performed by an experienced investigator using CAAS MRV 3.3 software (Pie Medical Imaging B.V.). Epicardial and endocardial LV myocardial contours (basal, midventricular, and apical slices) were manually traced to acquire intensity over time curves at rest and stress for 16 segments (segment 17, the LV apex, was not imaged). The calculated relative upslope (maximum upslope of the myocardial signal enhancement divided by the maximum upslope of the LV cavity signal enhancement) was used for the calculation of segmental MPRI. MPRI was defined as the ratio of relative upslope (stress) to relative upslope (rest), and segmental values were averaged. Our in-laboratory intrarater reliability for measuring MPRI, reported as a coefficient of variation, is 3.6%.[23] Delayed enhancement images were read by an experienced investigator to identify areas of regional fibrosis.

Statistical Analysis

Baseline characteristics are presented as mean±SD or proportions. Inferential data are reported as mean±SE, with differences between cases and controls compared using Student *t* tests. Normality was assessed by the Kolmogorov–Smirnov goodness-of-fit test. Multiple linear regression analysis was performed to assess the relationship between indices of diastolic function (peak circumferential strain and peak untwisting rate) and multiple patient characteristics (ie, age, body mass index, blood pressure, LV mass, heart rate, and global MPRI). In all cases, differences were considered significant if P values <0.05.

Results

Twenty cases and 15 age-matched controls underwent cardiac MRI with contrast. Subject characteristics are presented in the Table. By design, cases and controls were well matched for age and body mass index. No group differences in resting heart rate, blood pressure, LV mass, or LV concentricity (mass/

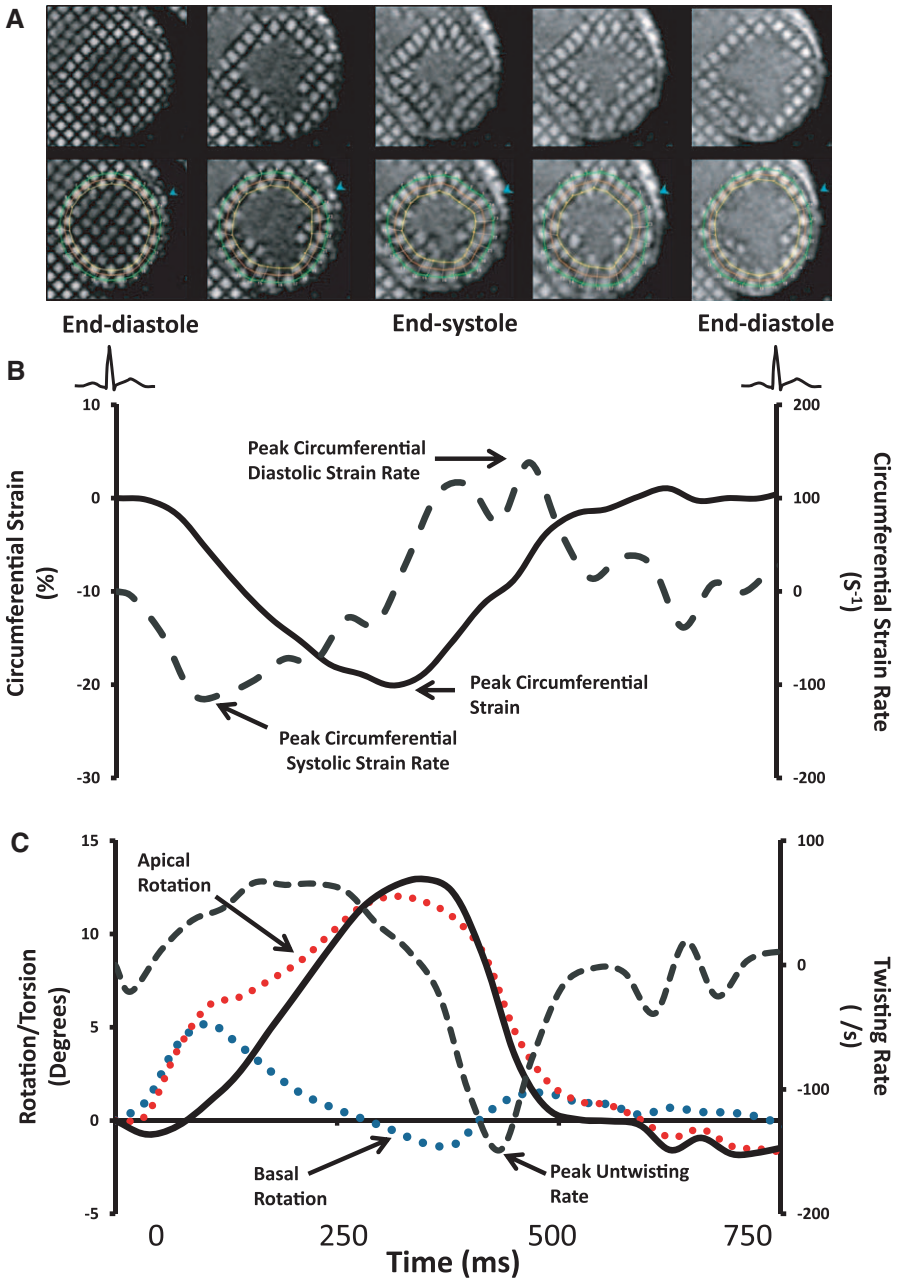

Figure 1. A, Representative cardiac magnetic resonance image obtained at the level of the papillary muscles, with a tissue tagging sequence (**top**). Analysis was performed using commercially available software (HARP; Diagnosoft), with user input limited to tracing the epicardium and endocardium of a single cardiac phase (end-systolic; **bottom**). The software then constructs a mesh, which tracks tissue deformation over a single cardiac cycle, using the harmonic phase. **B**, Representative tracing of circumferential strain (solid black line) and circumferential strain rate (dashed line) over a single cardiac cycle. **C**, Representative data tracing of apical (red line) and basal (blue line) rotation, net torsion (solid black line), and the rate of ventricular twisting (dashed line) over a single cardiac cycle.

end-diastolic volume) were found between the groups. Consistent with previous observations, 62% of the cases had a history of hypertension, although treated blood pressure was not different from the reference control group. Likewise, 62% of cases were also hyperlipidemic, and 19% had a history of type 2 diabetes mellitus. As expected, MPRI was lower in cases than in controls ($P<0.05$). We found no evidence of myocardial fibrosis (delayed enhancement) in any of the cases studied.

Preserved LV Systolic Function

LV global systolic function (ie, LV ejection fraction) was well preserved in cases compared with controls (see the Table). Likewise, circumferential strain (−20.7±0.6% versus −21.9±0.5%) and systolic circumferential strain rate (−105.9±6.1% versus −109.0±3.8% per second) were also found to be similar between cases and controls.

Impaired LV Diastolic Function

LV diastolic function was assessed in 3 ways. First, using tissue tagging, we assessed the peak rate of circumferential strain in diastole, which was found to be greatly impaired in cases versus controls (Figure 2). Second, also using tissue tagging, we assessed the peak rate of basal to apical rotation (ie, peak untwisting rate), demonstrating an impairment in cases compared with controls (Figure 2). Third, using conventional cinematic imaging, we assessed early peak filling rate. Unlike tissue tagging parameters, peak ventricular filling rate was found to be similar between cases and controls (356.4±27.5 versus 370.0±14.9 mL/s).

In addition to functional parameters of LV diastolic function, we also assessed the timing of each diastolic event. Cases and controls differed significantly with regard to the timing of specific diastolic event: (1) the timing of peak filling rate was

Table. Baseline Characteristics

Variable	Cases	Controls	*P* Value
N	20	15	…
Age, y	60	56	0.062
Height, cm	163.4±7.1	162.7±7.3	0.771
Weight, kg	73.8±16.2	69.1±16.2	0.406
Body mass index, kg/m^2	27.6±5.7	25.9±4.3	0.348
Hemodynamic parameters			
Heart rate, beats/min	66±10	62±6	0.231
Systolic blood pressure, mm Hg	134±19	124±15	0.099
Diastolic blood pressure, mm Hg	64±12	67±10	0.427
Mean arterial pressure, mm Hg	87±12	86±8	0.703
Ventricular function and geometry			
LV ejection fraction, %	63±2	65±6	0.849
LV end-diastolic volume, mL	126.1±24.5	126.0±20.0	0.984
LV end-systolic volume, mL	39.4±14.5	44.4±11.1	0.282
LV mass, g	90.7±12.8	83.8±12.6	0.131
LV mass/volume, g/mL	0.73±0.1	0.67±0.1	0.113
Coronary perfusion			
Global MPRI	1.88±0.49	2.20±0.53	0.037
Comorbidities, n			
History of hypertension	13	0	…
History of hyperlipidemia	14	0	…
History of type II diabetes mellitus	4	0	…
Current use of medications, n			
ACE-I or ARB	10	0	…
β-Blocker	12	0	…
Statin	14	0	…
Calcium channel blocker	12	0	…

Data reported as mean±SD unless otherwise specified. ACE-I indicates angiotensin-converting enzyme inhibitor; ARB, angiotensin receptor blocker; LV, left ventricular; and MPRI, myocardial perfusion reserve index.

202±9 ms in cases versus 162±9 ms in controls (*P*=0.003); (2) the time of peak diastolic circumferential strain rate was 500±9 ms in cases versus 472±10 ms in controls (*P*=0.053); and (3) the timing of peak ventricular untwisting rate was 416±13 ms in cases versus 374±9 ms in controls (*P*=0.036).

Lastly, we performed multiple linear regression analysis to assess whether diastolic function, measured by MR tissue tagging, was related to common cardiovascular risk factors. Diastolic circumferential strain rate and peak untwisting rate remained significantly different between groups, even after adjusting for cardiovascular risk factors (*P*=0.03 and 0.02, respectively). Neither diastolic circumferential strain rate nor peak untwisting rate were predicted by age, body mass index, arterial blood pressure, LV mass, LV concentricity, or resting heart rate. Moreover, diastolic dysfunction was not found to be related to MPRI.

Discussion

In women with signs and symptoms of ischemia in the absence of obstructive CAD, we observed differences in diastolic function—with preserved systolic function—compared with a group of age- and body mass index–matched controls. Our results were independent of common cardiovascular risk factors, including age, body mass index, hypertension, or LV hypertrophy.

Angina, an evidence of ischemia, in women is a major health problem, yet it remains underdiagnosed and undertreated.[19] One possible contributing factor may be our continued overreliance on global markers of cardiac function, such as ejection fraction or fractional shortening. It is now well established that patients presenting with symptoms of cardiac failure will often have normal LV ejection fractions. Thus, to achieve early, targeted treatment, more sensitive imaging modalities, which are capable of evaluating the entire cardiac cycle, are needed. Here, by using cardiac MR tissue tagging, we were able to detect diastolic differences in a cohort of women with signs and symptoms of ischemia but no obstructive CAD.

Cardiac MR tissue tagging provides 2 important measures of LV diastolic function: strain rate and the rate of ventricular untwisting. Diastolic strain rate reflects the rate of tissue deformation (ie, myocyte lengthening) during early diastole, similar to early myocardial tissue velocities measured by Doppler ultrasound. Unlike Doppler ultrasound, however, strain imaging provides more direct information about tissue lengthening and is less affected by the tethering of noncontracting cardiomyocytes or the Doppler insonation angle, thus making it a more superior measure of myocardial relaxation. LV untwisting occurs as a result of the left ventricle's unique helical fiber orientation,[24–27] which gives rise to basal-to-apical rotation/twisting during systole. During diastole, stored potential energy generated during systole is released as kinetic energy, resulting in early rapid ventricular untwisting. Indeed, the rate of ventricular untwisting is strongly associated with the transmitral pressure gradient[28–31] and the rate of isovolumic relaxation.[32] The seminal finding of this investigation was that both diastolic strain rate and peak LV untwisting rate are reduced in women with signs and symptoms of ischemia but no obstructive CAD.

We also assessed the rate of early LV filling by using cinematic imaging, which is similar to conventional mitral inflow velocimetry. In our hands, this conventional technique failed to detect differences in diastolic function between cases and controls. We think that this further highlights the added benefit of using newer, more sensitive MRI techniques, such as MR tissue tagging. Interestingly, cinematic imaging was able to detect a significant diastolic time delay in patients compared with controls, suggesting that it took longer to achieve a similar peak ventricular filling rate. This finding was also confirmed by tissue tagging.

Diastolic dysfunction is multifactorial and increasingly recognized as a major contributing factor of morbidity and mortality.[33,34] Factors such as cardiac hypertrophy, myocardial fibrosis, metabolic dysfunction of cardiomyocytes, or microvascular abnormalities have all been implicated. Our imaging studies ruled out cardiac hypertrophy as a major contributing mechanism because we found no difference in LV mass or LV concentricity between cases and controls. Myocardial fibrosis is also an unlikely contributing factor because none of the patients studied showed evidence of myocardial fibrosis on delayed enhancement imaging

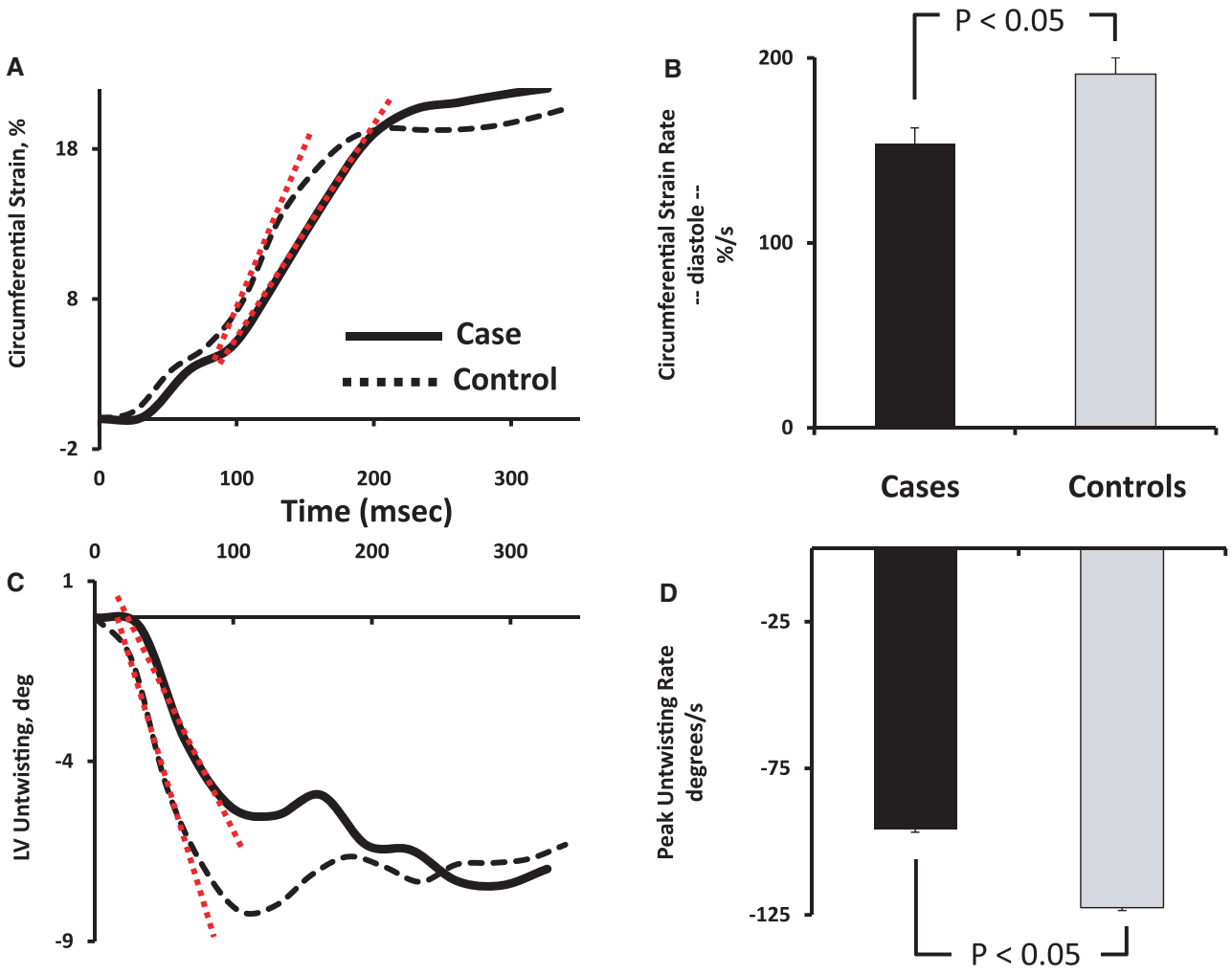

Figure 2. MR tissue tagging reveals differences in diastolic function in women with angina who were free from obstructive coronary artery disease (cases) and a group of age- and body mass index–matched reference controls (controls). **A**, Circumferential strain from a representative case (solid line) and a representative control (dashed line) subject. Time 0 represents end-systole. Red dashed line illustrates differences in the rate of relaxation. **B**, Summary data showing significant reductions in circumferential diastolic strain rate in cases compared with controls. **C**, Left ventricular (LV) torsion in a representative case (solid line) and a representative control (dashed line) subject. Time 0 represents end-systole. Red dashed line illustrates differences in the rate of ventricular untwisting. **D**, Summary data showing significant reductions in the rate of LV untwisting in cases compared with controls. Data are reported as mean±SE.

with gadolinium. Thus, although the current experimental approach does not allow us to completely differentiate changes in relaxation from that of compliance, the general absence of hypertrophy or fibrosis strongly suggests impairments in relaxation, rather than compliance per se. We hypothesize that diastolic dysfunction is secondary to the clustering of risk factors (eg, hypertension, diabetes mellitus, obesity) commonly observed in this syndrome.

The clinical significance of our results remains unclear. Diastolic heart failure, commonly referred to as heart failure with preserved ejection fraction, is an increasingly recognized entity with similar, if not worse, clinical outcomes compared with traditional heart failure with reduced ejection fraction.[33,34] Older women with ≥1 Framingham risk factors are often the group affected by heart failure with preserved ejection fraction and make up the bulk majority of our population. Indeed, we have also observed a relatively high proportion of new-onset heart failure hospitalizations and nonfatal myocardial infarctions in this population.[1] It is, therefore, interesting to speculate that our observations provide important subclinical insight into a group of patients destined for heart failure. Perhaps early identification of cardiac abnormalities with such sensitive imaging techniques as performed here provides an important treatment window to prevent/rescue disease progression.

Limitations

Conventional Doppler ultrasound was not performed in the present investigation to assess diastolic function, which limits the clinical applicability. However, as discussed, we consider strain imaging to be a more robust measure of diastolic function. Of course, speckle-tracking echocardiography can also provide similar strain information, with similar sensitivity and variability as MRI. However, because our study also included LV morphology and myocardial perfusion measurements (where MRI is clearly superior to echocardiography),

it followed that MR tissue tagging was the best modality to assess LV strain and strain rate in this investigation.

Because of MR tag fading, we acquired 2 sets of images at each short-axis location to ensure optimal tag quality during each phase of the cardiac cycle (systole and diastole). Although other imaging protocols may generate tags that persist with good signal-to-noise throughout the entire cardiac cycle (eg, complimentary spatial modulation of magnetization), acquisition time and breath-hold time are still doubled, and these techniques can be susceptible to image misregistration.

Because women with ischemic heart disease tend to have a clustering of risk factors, including obesity, hypertension, and dyslipidemia, future studies will need to include an additional referent group of women with underlying comorbidities but without myocardial ischemia. Indeed, although the 2 groups in the present study shared similar LV geometries and blood pressure, we cannot completely rule out the possibility that additional underlying comorbidities may have contributed to the present results.

In conclusion, women with signs and symptoms of ischemia in the absence of obstructive CAD have abnormalities in diastolic function, as assessed by high-resolution cardiac MRI. This hypothesis-generating study provides encouraging insight into the pathophysiology of this disease and opens new opportunities for future studies to explore specific mechanisms as well as potential treatment options—both on acute effectiveness and long-term survival.

Sources of Funding

This work was supported by contracts from the National Heart, Lung, and Blood Institute (N01-HV-68161, N01-HV-68162, N01-HV-68163, N01-HV-68164); grants U0164829, U01 HL649141, U01 HL649241, T32HL69751, 1R03AG032631 from the National Institute on Aging; K23HL105787, GCRC grant MO1-RR00425 from the National Center for Research Resources UN55ES6580F; and grants from the Gustavus and Louis Pfeiffer Research Foundation (Danville, NJ), The Women's Guild of Cedars-Sinai Medical Center (Los Angeles, CA), The Ladies Hospital Aid Society of Western Pennsylvania (Pittsburgh, PA), QMED, Inc (Laurence Harbor, NJ), the Edythe L. Broad Women's Heart Research Fellowship, Cedars-Sinai Medical Center (Los Angeles, CA), the Barbra Streisand Women's Cardiovascular Research and Education Program, the Linda Joy Pollin Women's Heart Health Program, Cedars-Sinai Medical Center (Los Angeles, CA), Cardium Therapeutics, Siemens, GE/Amersham, Astellas, Lantheus, Spectrum Dynamics, and Iba Molecular. M.D.N. was the recipient of research fellowship grants from the Heart and Stroke Foundation of Canada and the Canadian Institutes for Health Research.

Disclosures

None.

References

1. Gulati M. Adverse cardiovascular outcomes in women with nonobstructive coronary artery disease: a report from the Women's Ischemia Syndrome Evaluation study and the St James Women Take Heart Project. *Arch Intern Med*. 2009;169:843–850.
2. Shaw LJ, Merz CN, Pepine CJ, Reis SE, Bittner V, Kip KE, Kelsey SF, Olson M, Johnson BD, Mankad S, Sharaf BL, Rogers WJ, Pohost GM, Sopko G; Women's Ischemia Syndrome Evaluation (WISE) Investigators. The economic burden of angina in women with suspected ischemic heart disease: results from the National Institutes of Health–National Heart, Lung, and Blood Institute–sponsored Women's Ischemia Syndrome Evaluation. *Circulation*. 2006;114:894–904.
3. Merz CN, Kelsey SF, Pepine CJ, Reichek N, Reis SE, Rogers WJ, Sharaf BL, Sopko G. The Women's Ischemia Syndrome Evaluation (WISE) study: protocol design, methodology and feasibility report. *J Am Coll Cardiol*. 1999;33:1453–1461.
4. Buchthal SD, den Hollander JA, Merz CN, Rogers WJ, Pepine CJ, Reichek N, Sharaf BL, Reis S, Kelsey SF, Pohost GM. Abnormal myocardial phosphorus-31 nuclear magnetic resonance spectroscopy in women with chest pain but normal coronary angiograms. *N Engl J Med*. 2000;342:829–835.
5. Reis SE, Holubkov R, Lee JS, Sharaf B, Reichek N, Rogers WJ, Walsh EG, Fuisz AR, Kerensky R, Detre KM, Sopko G, Pepine CJ. Coronary flow velocity response to adenosine characterizes coronary microvascular function in women with chest pain and no obstructive coronary disease: results from the pilot phase of the Women's Ischemia Syndrome Evaluation (WISE) study. *J Am Coll Cardiol*. 1999;33:1469–1475.
6. von Mering GO, Arant CB, Wessel TR, McGorray SP, Bairey Merz CN, Sharaf BL, Smith KM, Olson MB, Johnson BD, Sopko G, Handberg E, Pepine CJ, Kerensky RA; National Heart, Lung, and Blood Institute. Abnormal coronary vasomotion as a prognostic indicator of cardiovascular events in women: results from the National Heart, Lung, and Blood Institute-Sponsored Women's Ischemia Syndrome Evaluation (WISE). *Circulation*. 2004;109:722–725.
7. Wong T, Klein R, Sharrett A. Retinal arteriolar narrowing and risk of coronary heart disease in men and women: the atherosclerosis risk in communities study. *JAMA*. 2002; 287:1153–1159.
8. Pepine CJ, Anderson RD, Sharaf BL, Reis SE, Smith KM, Handberg EM, Johnson BD, Sopko G, Bairey Merz CN. Coronary microvascular reactivity to adenosine predicts adverse outcome in women evaluated for suspected ischemia results from the National Heart, Lung and Blood Institute WISE (Women's Ischemia Syndrome Evaluation) study. *J Am Coll Cardiol*. 2010;55:2825–2832.
9. Burke AP, Farb A, Malcom GT, Liang Y, Smialek J, Virmani R. Effect of risk factors on the mechanism of acute thrombosis and sudden coronary death in women. *Circulation*. 1998;97:2110–2116.
10. Burke AP, Virmani R, Galis Z, Haudenschild CC, Muller JE. 34th Bethesda Conference: Task force #2–What is the pathologic basis for new atherosclerosis imaging techniques? *J Am Coll Cardiol*. 2003;41:1874–1886.
11. Zerhouni EA, Parish DM, Rogers WJ, Yang A, Shapiro EP. Human heart: tagging with MR imaging: a method for noninvasive assessment of myocardial motion. *Radiology*. 1988;169:59–63.
12. Yeon SB, Reichek N, Tallant BA, Lima JA, Calhoun LP, Clark NR, Hoffman EA, Ho KK, Axel L. Validation of *in vivo* myocardial strain measurement by magnetic resonance tagging with sonomicrometry. *J Am Coll Cardiol*. 2001;38:555–561.
13. Aurigemma GP, Silver KH, Priest MA, Gaasch WH. Geometric changes allow normal ejection fraction despite depressed myocardial shortening in hypertensive left ventricular hypertrophy. *J Am Coll Cardiol*. 1995;26:195–202.
14. El-Menyar AA, Galzerano D, Asaad N, Al-Mulla A, Arafa SE, Al Suwaidi J. Detection of myocardial dysfunction in the presence of normal ejection fraction. *J Cardiovasc Med (Hagerstown)*. 2007;8:923–933.
15. Azevedo CF, Amado LC, Kraitchman DL, Gerber BL, Osman NF, Rochitte CE, Edvardsen T, Lima JA. Persistent diastolic dysfunction despite complete systolic functional recovery after reperfused acute myocardial infarction demonstrated by tagged magnetic resonance imaging. *Eur Heart J*. 2004;25:1419–1427.
16. Garot J. The study of diastole by tagged MRI: are we nearly there yet? *Eur Heart J*. 2004;25:1376–1377.
17. Grundy SM, Bilheimer D, Chait A, Clark LT, Denke M, Havel RJ, Hazzard WR, Hulley SB, Hunninghake DB, Kreisberg RA, KrisEtherton P, McKenney JM, Newman MA, Schaefer EJ, Sobel BE, Somelofski C, Weinstein MC, Brewer HB Jr, Cleeman JI, Donato KA, Ernst N, Hoeg JM, Rifkind BM, Rossouw J, Sempos CT, Gallivan JM, Harris MN, Quint-Adler L. Summary of the second report of the national cholesterol education program (ncep) expert panel on detection, evaluation, and treatment of high blood cholesterol in adults (adult treatment panel ii). *JAMA*. 1993;269:3015–3023.
18. Attili AK, Schuster A, Nagel E, Reiber JH, van der Geest RJ. Quantification in cardiac MRI: advances in image acquisition and processing. *Int J Cardiovasc Imaging*. 2010;26(suppl 1):27–40.
19. Doyle M, Fuisz A, Kortright E, Biederman RW, Walsh EG, Martin ET, Tauxe L, Rogers WJ, Merz CN, Pepine C, Sharaf B, Pohost GM. The impact of myocardial flow reserve on the detection of coronary artery disease by perfusion imaging methods: an NHLBI WISE study. *J Cardiovasc Magn Reson*. 2003;5:475–485.

20. Zeidan Z, Erbel R, Barkhausen J, Hunold P, Bartel T, Buck T. Analysis of global systolic and diastolic left ventricular performance using volume-time curves by real-time three-dimensional echocardiography. *J Am Soc Echocardiogr*. 2003;16:29–37.
21. Cain PA, Ahl R, Hedstrom E, Ugander M, Allansdotter-Johnsson A, Friberg P, Arheden H. Age and gender specific normal values of left ventricular mass, volume and function for gradient echo magnetic resonance imaging: a cross sectional study. *BMC Med Imaging*. 2009;9:2.
22. Maceira AM, Prasad SK, Khan M, Pennell DJ. Normalized left ventricular systolic and diastolic function by steady state free precession cardiovascular magnetic resonance. *J Cardiovasc Magn Reson*. 2006;8:417–426.
23. Goykhman P, Mehta PK, Agarwal M, Shufelt C, Slomka PJ, Yang Y, Xu Y, Shaw LJ, Berman DS, Merz NB, Thomson LE. Reproducibility of myocardial perfusion reserve: variations in measurements from post processing using commercially available software. *Cardiovasc Diagn Ther*. 2012;2:268–277.
24. Streeter DD Jr, Spotnitz HM, Patel DP, Ross J Jr, Sonnenblick EH. Fiber orientation in the canine left ventricle during diastole and systole. *Circ Res*. 1969;24:339–347.
25. Rushmer RF, Crystal DK, Wagner C. The functional anatomy of ventricular contraction. *Circ Res*. 1953;1:162–170.
26. Greenbaum RA, Ho SY, Gibson DG, Becker AE, Anderson RH. Left ventricular fibre architecture in man. *Br Heart J*. 1981;45:248–263.
27. Sengupta PP, Krishnamoorthy VK, Korinek J, Narula J, Vannan MA, Lester SJ, Tajik JA, Seward JB, Khandheria BK, Belohlavek M. Left ventricular form and function revisited: applied translational science to cardiovascular ultrasound imaging. *J Am Soc Echocardiogr*. 2007;20:539–551.
28. Moon MR, Ingels NB Jr, Daughters GT II, Stinson EB, Hansen DE, Miller DC. Alterations in left ventricular twist mechanics with inotropic stimulation and volume loading in human subjects. *Circulation*. 1994;89:142–150.
29. Gibbons Kroeker CA, Ter Keurs HE, Knudtson ML, Tyberg JV, Beyar R. An optical device to measure the dynamics of apex rotation of the left ventricle. *Am J Physiol*. 1993;265(4 Pt 2):H1444–H1449.
30. Notomi Y, Martin-Miklovic MG, Oryszak SJ, Shiota T, Deserranno D, Popovic ZB, Garcia MJ, Greenberg NL, Thomas JD. Enhanced ventricular untwisting during exercise: a mechanistic manifestation of elastic recoil described by Doppler tissue imaging. *Circulation*. 2006;113:2524–2533.
31. Rademakers FE, Buchalter MB, Rogers WJ, Zerhouni EA, Weisfeldt ML, Weiss JL, Shapiro EP. Dissociation between left ventricular untwisting and filling. Accentuation by catecholamines. *Circulation*. 1992;85:1572–1581.
32. Dong SJ, Hees PS, Siu CO, Weiss JL, Shapiro EP. MRI assessment of LV relaxation by untwisting rate: a new isovolumic phase measure of tau. *Am J Physiol Heart Circ Physiol*. 2001;281:H2002–H2009.
33. Owan TE, Hodge DO, Herges RM, Jacobsen SJ, Roger VL, Redfield MM. Trends in prevalence and outcome of heart failure with preserved ejection fraction. *N Engl J Med*. 2006;355:251–259.
34. Aljaroudi W, Alraies MC, Halley C, Rodriguez L, Grimm RA, Thomas JD, Jaber WA. Impact of progression of diastolic dysfunction on mortality in patients with normal ejection fraction. *Circulation*. 2012;125:782–788.

CLINICAL PERSPECTIVE

This study used cardiac magnetic resonance tissue tagging to test the hypothesis that left ventricular diastolic function is impaired in a cohort of women with signs and symptoms of ischemia in the absence of obstructive coronary artery disease. We observed significant reductions in both diastolic circumferential strain rate and peak left ventricular untwisting rate. This is the first study to demonstrate diastolic dysfunction in women with signs and symptoms of ischemia in the absence of coronary artery disease and sets the stage for future studies to address specific mechanisms of action and evaluate potential therapeutic countermeasures.